Effects of the microRNA-99a-5p/VLDLR axis in lung cancer cell sensitivity to chemotherapy and its mechanism

Yaoguo Lang[1], Xianglong Kong[1], Benkun Liu[1], Xiangyuan Jin[1], Lantao Chen[1], Shidong Xu[1]*

[1]*Department of Thoracic Surgery, Harbin Medical University Cancer Hospital, Heilongjiang, China*

Lung cancer is a major cause of cancer-related death worldwide. This study investigated the regulatory effects of the microRNA-99a-5p (miR-99a-5)/VLDLR axis on lung cancer cell sensitivity to chemotherapy and its mechanism. miR-99a-5p and VLDLR expression levels were quantified using RT-qPCR and western blotting, respectively. The IC50 value of cisplatin (DDP) was determined using a CCK-8 assay. Lung cancer cell proliferation and apoptosis were measured using the CCK-8 assay and flow cytometry, respectively. The mRNA expression levels of apoptosis-related factors (Bax, Bcl-2, and Caspase-3) were evaluated using RT-qPCR. The direct relationship between miR-99a-5p and VLDLR was validated using dual-luciferase reporter gene and RIP assays. miR-99a-5p was weakly expressed in DDP-resistant lung cancer cells. Overexpression of miR-99a-5p promoted DDP sensitivity, suppressed proliferation and colony formation, and promoted apoptosis of A549/DDP cells *in vitro*. Mechanistically, miR-99a-5p restrained VLDLR expression by binding to VLDLR 3'UTR, and miR-99a-5p mediated inhibition of VLDLR regulated the DDP sensitivity, proliferation, and apoptosis of A549/DDP cells. Overexpression of miR-99a-5p inhibited the growth of A549 cells and increased chemosensitivity of A549 cells to DDP *in vivo*. In conclusion, miR-99a-5p overexpression promotes sensitivity to DDP and cell apoptosis by downregulating VLDLR expression in A549/DDP cells.

Keywords: Lung cancer. MicroRNA-99a-5. VLDLR. Cisplatin. Proliferation. Colony formation. Apoptosis.

INTRODUCTION

Lung cancer is a common type of cancer and one of the leading causes of increasing mortality (Thakur, Singh, Choudhary, 2020). Multiple options are available for lung cancer therapy, including surgery, radiation therapy, and chemotherapy (Yang *et al.*, 2020). Chemotherapy remains the preferred treatment modality for lung cancer and can prolong patient survival by effectively controlling tumor development (Yu, Jin,

Shou, 2021). However, in many cases, cancer cells develop drug resistance and become unresponsive to chemotherapy (El-Hussein *et al.*, 2021). Cisplatin (DDP) is a cell cycle-non-specific cytotoxic drug that primarily targets DNA (Tang, Yang, Zhou, 2011). DDP is a common chemotherapeutic agent that has shown excellent clinical efficacy (Ashrafizadeh *et al.*, 2021). DDP administration represses growth and induces apoptotic body formation and apoptosis in A549 cells (Teng *et al.*, 2018). In addition, it has been reported that DDP is an effective broad-spectrum anticancer drug and can be used in the treatment of lung cancer. Dysregulation of microRNAs (miRNAs) has been linked to chemoresistance of tumor cells to DDP (Chen *et al.*, 2015).

miRNAs function as post-transcriptional regulators of gene expression. Moreover, miRNAs powerfully modulate various cellular activities such as cell growth, apoptosis, and differentiation (Saliminejad et al., 2019). It has also been shown that miRNAs play a key role in regulating biological processes and pathways, leading to significant physiological effects (Hwang, Chang, Baek, 2023). In addition, miRNAs exhibit abnormal expression levels in lung cancer and influence its initiation and progression (Li et al., 2022). Furthermore, it has been suggested that miRNAs, as endogenous inhibitors of target mRNAs, are strongly associated with each step of non-small cell lung cancer (NSCLC) growth, ranging from tumor initiation to progression and metastasis (Ahn, Ko, 2020). miR-99a-5p is linked to the pathogenesis of various disorders (Gu, Bao, 2022). For example, miR-99a-5p regulates cervical cancer (CC) cell apoptosis and glycolysis, thereby offering a potential therapeutic target for CC (Wang et al., 2022). miR-99a-5p possesses a potential diagnostic function, even in detecting early breast cancer, and has been proved to act as a promising non-invasive biomarker for detecting breast cancer (Garrido-Cano et al., 2020). Furthermore, miR-99a-5p participates in lung adenocarcinoma (LUAD) cell proliferation, demonstrating its tumor-suppressive role (Mizuno et al., 2020; Zheng et al., 2022). Very low-density lipoprotein receptor (VLDLR) belongs to the low-density lipoprotein receptor family, and has been detected in various cancers to date (Luo et al., 2010). VLDLR is regarded as a multifunctional receptor because of its binding to many ligands, role in endocytosis, and regulation of cellular signaling (He et al., 2010). VLDLR may be a crucial target for breast cancer treatment (Yang et al., 2022). Furthermore, increasing evidence has shown that VLDLR alters expression and might function in tumor development by impacting cell metastasis and proliferation (Kim et al., 2017). Nevertheless, the precise function of the miR-99a-5/VLDLR axis in lung cancer remains unclear. Therefore, this study aimed to explore the regulatory effects and mechanisms of the miR-99a-5/VLDLR axis on lung cancer cell sensitivity to chemotherapy, thus providing a novel direction for lung cancer treatment.

MATERIAL A ND METHODS

Ethics statement

This research for clinical samples was confirmed by the Ethic Committee of our hospital and all patients signed the written informed consent. This research followed the Declaration of Helsinki. The animal care procedures and animal experiments in the research were conducted under ratification of the Animal Ethic Committee of our hospital.

Clinical tissues

Cancerous and adjacent normal tissues were obtained from 86 patients with lung cancer who underwent surgical resection at our hospital. All cancerous tissue specimens were diagnosed as lung cancer by pathological examination. All fresh samples were quick-frozen and stored in liquid nitrogen for future experiments.

Cell transfection

The miR-99a-5p inhibitor, miR-99a-5p mimic and their corresponding negative controls (NCs), small interfering RNAs against VLDLR (si-VLDLR), and its corresponding NCs (si-NC) were supplied by GenePharma (Shanghai, China). Cells were inoculated into 6-well plates at a cell density of 70%–80%, and Lipofectamine 3000 (Invitrogen) and Opti-MEM (Gibco) were used for transfection. The miR-99a-5p inhibitor (50 nM), miR-99a-5p mimic (50 nM), and si-VLDLR (100 nM) (Liu et al., 2013) were dissolved in Opti-MEM supplemented with diluted Lipofectamine 3000 and incubated for 5 min at room temperature. The cells were then supplemented with these mixtures and serum-free medium.

Reverse transcription-quantitative polymerase chain reaction (RT-qPCR)

Total RNA was extracted using a TRIzol Kit (Invitrogen). The mRNA was reverse-transcribed using PrimeScript RT Master Mix (Takara, Dalian, China) to obtain cDNA, and miR-99a-5p was reverse-transcribed

into cDNA using a Mir-X miRNA First-Strand Synthesis Kit (Takara). SYBR® Premix Ex TaqTM II Kit (Takara) was utilized to perform RT-qPCR in a real-time fluorescence qPCR instrument (ABI 7500, ABI, Foster City, CA, USA). The related primers were synthesized by Sangon (Shanghai, China) (primer sequences are displayed in Supplementary Table I). U6 was used as the internal reference for miR-99a-5p, and β-actin was used as the internal reference for the remaining mRNAs. The products' relative expression was calculated using the $2^{-\Delta\Delta Ct}$ method (Livak, Schmittgen, 2001).

Western blot analysis

Transfected cells were lysed using radioimmunoprecipitation assay (RIPA) Protein Lysis Solution (Beyotime, Shanghai, China), and a BCA Quantification Kit (Beyotime) was used to quantify protein concentrations. After quantification, these proteins were supplemented with loading buffer and subjected to heating at 95°C for 5 min. An equal amount of protein (50 µg protein/lane) was separated by sodium dodecyl sulfate polyacrylamide gel electrophoresis (SDS-PAGE) and transferred to polyvinylidene difluoride (PVDF) membranes, which were blocked with 5% non-fat milk for 1 h at room temperature, and probed with primary antibodies VLDLR (ab203271, 1:1000, Abcam, Cambridge, UK) and β-actin (ab5694, 1:500, Abcam). Next, the membranes were incubated with horseradish peroxidase-labeled secondary antibody goat anti-rabbit IgG H&L (HRP) (ab6721, 1:5000, Abcam) and hybridized for 2 h at ambient temperature. The blots were visualized using an enhanced chemiluminescence reaction (ECL) system and densitometric analysis was performed using Quantity One software (Bio-Rad).

CCK-8 assay

Cell viability was assessed using a CCK-8 Kit (Beyotime). After digestion with trypsin, the cells were re-suspended and inoculated with cell suspensions (1×10^4 cells/well) in 96-well plates, and incubated for 24 h in an incubator. Each well was cultivated for 4 h with 10 µL of CCK-8 solution. A microplate reader was used to measure the absorbance at 450 nm. Cellular viability (%) = [(As-Ab)/(Ac-Ab)] × 100%, where As is the absorbance of study wells, Ac is the absorbance of control wells, and Ab is the absorbance of blank wells.

DDP resistance was measured by adding DDP (0.25, 0.5, 1, 2, 4, 8, or 16 µg/mL) (Xie *et al.*, 2022) to inoculated cells. The absorbance was measured, and the semi-inhibitory concentration IC50 was calculated to quantify or measure the cell sensitivity to DDP. The IC50 value was calculated as 50% inhibition of cell viability by DDP, with a higher IC50 value indicating a higher resistance potential.

Clone formation assay

The transfected cells in each group were trypsin-digested, inoculated (5×10^2 cells/well) into 6-well plates, and incubated for 2–3 weeks. Visible colonies were fixed with 4% paraformaldehyde for 10 min at ambient temperature and stained with 0.1% crystal violet at ambient temperature for 10 min. Stained colonies were counted under a microscope.

Flow cytometry

Annexin V-FITC/propidium iodide (PI) staining was used to detect apoptosis. The cells in each group were digested into individual cell suspension, and the cell suspension (100 µL) was re-suspended in binding buffer (200 µL). Next, the cells were stained with 10 µL Annexin V-FITC and 5 µL PI (BD Biosciences, San Diego, CA, USA) at room temperature for 15 min in the dark. The binding buffer (300 µL) was added, and flow cytometry was performed to evaluate cell apoptosis at an excitation wavelength of 488 nm (Cai *et al.*, 2019).

Dual-luciferase assay

The binding sites of miR-99a-5p and VLDLR were predicted using the StarBase database (http://starbase.sysu.edu.cn/). Recombinant luciferase reporter gene vectors containing binding sites (VLDLR-WT) and mutant binding sites (VLDLR-Mut) were constructed and co-transfected with the miR-99-5p mimic and mimic

NC into A549 cells for a dual luciferase reporter gene assay. After transfection, cells were collected and lysed for 48 h. A dual-luciferase reporter gene analysis system (Promega, Madison, WI, USA) was used to measure the relative luciferase activity, with Renilla luciferase as an internal reference (Gao *et al.*, 2019).

RIP assay

The Magna RIP™ RNA Binding Protein Immunoprecipitation Kit (Millipore, Billerica, MA, USA) was used to conduct the RIP assay. The cell lysates were grouped into two equal parts and one group was cultured with Argonaute-2 (Ago2, ab186733, Abcam) antibodies and the other with Immunoglobulin G (IgG, ab172730, Abcam) antibodies. The mixture was then supplemented with agarose beads (Bio-Rad Laboratories) and incubated. The enrichment of miR-99a-5p and VLDLR in the beads was analyzed using RT-qPCR (Ding *et al.*, 2020).

Chemotherapy sensitivity assay in nude mouse transplanted models

Twenty-four BALB/c nude mice (4–6 weeks old, weighing 18–25 g) were kept in a constant temperature of 25–27°C with constant humidity. The mice were randomly divided into four groups: miR-NC, miR-99a-5p, miR-NC + DDP, and miR-99a-5p + DDP, with six mice per group. A549 cells with stable overexpression of miR-99a-5p or scramble miRNA were resuspended in PBS and 1×10^6 cells (200 µl) (Yu *et al.*, 2017) were subcutaneously inoculated on the back of nude mice to establish nude mouse transplanted tumor models. When the tumor volume reached 0.1 cm^3, mice in the miR-NC + DDP and miR-99a-5p + DDP groups were injected with DDP (3 mg/kg) once a week for four weeks. Throughout the treatment period, the longest and shortest tumor diameters were measured weekly using Vernier calipers, and the tumor volume was calculated as (a × b^2)/2 (a is the longest diameter of the tumor and b is the shortest diameter). Tumor growth curves were plotted according to the changes in tumor volume. After four weeks, the nude mice were intraperitoneally injected with an overdose of pentobarbital sodium (100 mg/kg)

for euthanasia, the subcutaneously transplanted tumors were stripped, and the weight of the tumor was recorded (Feng *et al.*, 2019).

TUNEL staining

Nude mouse tumor tissues were fixed in 4% paraformaldehyde overnight, then embedded in paraffin, and subsequently, the embedded tissues were cut. The tissue sections were dewaxed and put into water with a dropwise addition of 50 µL 1% proteinase K dilution, followed by a 30 min incubation in a 37□ thermostat. The sections were added with methanolic solution containing 0.3% H$_2$O$_2$ in order to eliminate endogenous POD activity, incubated at 37□ for 30 min at room temperature, and dropwise supplemented with TUNEL reaction solution. The sections were then subjected to TdT enzyme culture, horseradish-labeled streptavidin incubation, 15 min incubation at room temperature with dropwise addition of DAB chromogenic solution, hematoxylin re-staining of nuclei, dehydration and permeabilization, and neutral gum sealing. An optical microscope was employed for photography, and five fields of view were randomly selected from each section. The number of positive cells and total cells in each view were counted using Image-Pro Plus 6.0 software. Apoptosis-positive cells had yellow or brown nuclei. TUNEL-positive cell rate was defined as the number of brown-positive cells/total number of cells.

Statistics

SPSS 21.0 statistical software (IBM SPSS Statistics, Chicago, IL, USA) and GraphPad Prism 8.0 software (GraphPad Software Inc., San Diego, CA, USA) were employed for data processing and graphing. Measurement data were expressed as mean ± standard deviation. The Kolmogorov-Smirnov normality test was utilzied to assess the data for normal distribution prior to analysis, while the Levene's test was employed to evaluate homogeneous variance assumption. For the data in a normal distribution and homogeneity of variance, comparisons between two groups were conducted by the t-test was applied, while comparisons among multiple groups were carried out by one-way analysis of

variance (ANOVA) or two-way ANOVA, with Tukey's multiple comparisons test for post hoc tests. $P < 0.05$ demonstrated a statistically significant difference.

RESULTS

miR-99a-5p expression is reduced in lung cancer

The UALCAN website was used to retrieve The Cancer Genome Atlas (TCGA) data to screen for lung cancer-related miRNA expression information, and the findings revealed that miR-99a was expressed at low levels in lung cancer (Figure 1A). In addition, clinically confirmed lung cancer tissues and control tissues were collected to assess the expression of miR-99a-5p in adjacent normal tissues and lung cancer tissues using RT-qPCR. The results showed that miR-99a-5p was expressed at low levels in lung cancer tissues (Figure 1B).

Furthermore, miR-99a-5p expression and its prognostic value in lung cancer were investigated (FIGURE 1C), and a reduction in miR-99a-5p levels was associated with poor survival in lung cancer patients.

To observe miR-99a-5p expression in lung cancer cells, RT-qPCR was conducted to assess miR-99a-5p expression levels in A549/DPP and parental A549 cells. The results revealed that miR-99a-5p expression was lower in A549 cells than in normal BEAS-2B cells. The expression of miR-99a-5p in A549/DPP cells was downregulated compared to that in parental A549 cells (Figure 1D). Subsequently, A549/DPP cell viability at different DDP concentrations was verified by the CCK-8 assay; the growth curve showed that the DDP IC$_{50}$ in A549/DPP cells was elevated in contrast to that of parental-sensitive cells, and the resistance index (RI) was approximately 15.40 (Figure 1E). These results suggest that miR-99a -5p may regulate DDP resistance in lung cancer cells.
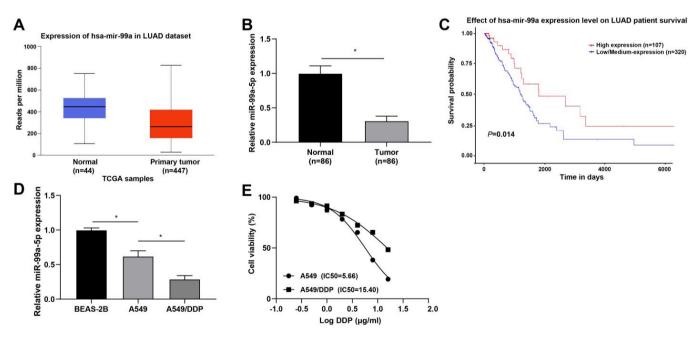

FIGURE 1 - The expression of miR-99a-5p is reduced in lung cancer. A. miR-99a-5p expression data in lung cancer were analyzed through the UALCAN-TCGA database; B. The expression of miR-99a-5p in adjacent normal tissues and lung cancer tissues was tested by RT-qPCR (n = 86); C. The relationship between miR-99a-5p expression and lung cancer prognosis was analyzed by UALCAN-TCGA database; D. The expression of miR-99a-5p in A549/DPP cells and A549 cells was measured by RT-qPCR; E. DPP-resistant cell line A549/DPP cell viability at different DDP concentrations was assessed by CCK-8 assay; *$P < 0.05$.

Overexpression of miR-99a-5p enhances sensitivity to DDP in lung cancer cells

To assess the effects of miR-99a-5p overexpression on the sensitivity of lung cancer cells to chemotherapy, the NC and miR-99a-5p mimics were transfected into A549/DDP cells. miR-99a-5p expression in the transfected cells was first tested using RT-qPCR, and the results showed that the expression of miR-99a-5p was higher after miR-99a-5p mimic transfection (Figure 2A). The cell viability at different DDP concentrations after mimic NC and miR-99a-5p mimic transfection was tested using the CCK-8 assay, and it was found that miR-99a-5p mimic transfection contributed to a lower cell viability and DDP IC_{50} value (Figure 2B).

In addition, cell proliferation, colony formation, and apoptosis were detected by CCK-8, colony formation, and flow cytometry assays, respectively, and the results indicated that after miR-99a-5p mimic transfection, cell proliferation and colony formation capacities were reduced (Figure 2C-D) while apoptosis was increased (Figure 2E). Finally, the expression levels of apoptosis-related genes (Bax, Bcl-2, and caspase-3) were assessed by RT-qPCR (Figure 2F), which revealed that Bax and caspase-3 mRNA expression levels were upregulated, and Bcl-2 mRNA expression levels were downregulated after miR-99a-5p mimic treatment.
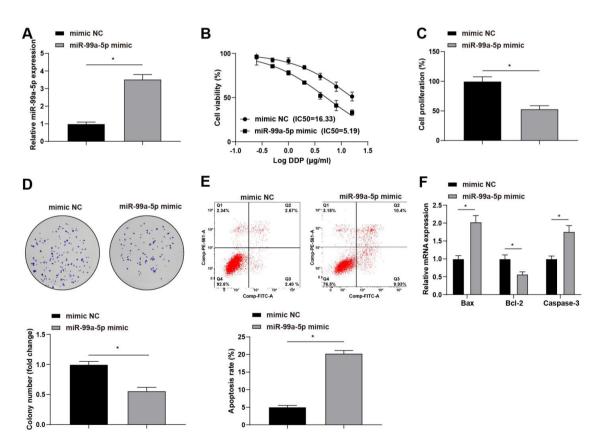

FIGURE 2 - Overexpression of miR-99a-5p promotes lung cancer cell chemotherapy sensitivity. A. miR-99a-5p expression levels in A549/DDP cells after transfected with miR-99a-5p mimic were measured by RT-qPCR; B. A549/DDP cell viability at different DDP concentrations after miR-99a-5p mimic transfection was tested by CCK-8 assay; C. The proliferation viability of A549/DDP cells after miR-99a 5p mimic transfection was determined by CCK-8 assay; D. The number of colonies in A549/DDP cells after miR-99a-5p mimic transfection was tested by colony formation assay; E. The apoptosis of A549/DDP cells after miR-99a-5p mimic transfection was assessed by flow cytometry assay; F. The expression levels of apoptosis-related genes Bax, Bcl-2, and caspase-3 in A549/DDP cells after transfection with miR-99a-5p mimic were tested by RT-qPCR; *$P < 0.05$.

miR-99a-5 targets and regulates VLDLR

To investigate the downstream regulatory mechanism of miR-99a-5p, we predicted the binding sites for miR-99a-5p in the VLDLR mRNA 3'UTR sequences through the Starbase database (http://starbase.sysu.edu.cn/) (Figure 3A), which indicated that VLDLR may be directly regulated by miR-99a-5p. To further verify this prediction, a dual-luciferase assay was performed, and it was found that after miR-99a-5p mimic transfection, the luciferase activity of the VLDLR-WT recombinant vectors was reduced (Figure 3B). RIP assay results indicated that Ago2, relative to IgG, could enrich higher levels of miR-99a-5p and VLDLR, which was consistent with the results of a dual-luciferase assay (Figure 3C).

Furthermore, VLDLR expression levels in clinical tissues were tested using RT-qPCR, which revealed upregulated VLDLR expression in lung cancer tissues (Figure 3D). The cellular assay also demonstrated that, compared to normal lung cells, VLDLR levels were increased in A549 cells and were more significantly elevated in A549/DPP cells (Figure 3E). Meanwhile, VLDLR expression levels in lung cancer cells after miR-99a-5p mimic and miR-99a-5p inhibitor transfection were assessed by western blotting. We found that VLDLR protein levels were decreased after treatment with the miR-99a-5p mimic, which was increased after miR-99a-5p inhibitor treatment (Figure 3F).
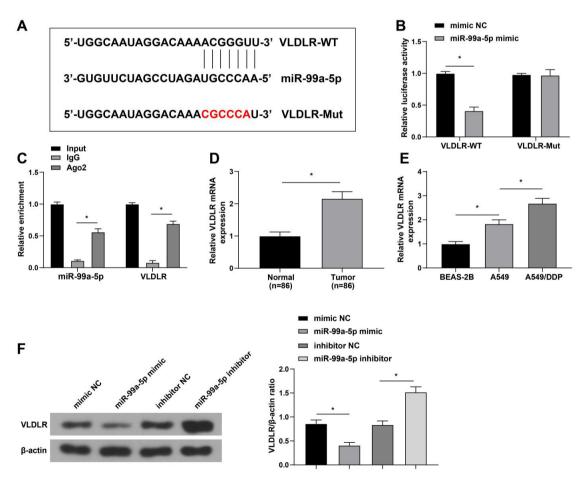

FIGURE 3 - miR-99a-5 targets and regulates VLDLR. A. The StarBase database predicted the binding sites between miR-99a-5p and VLDLR; B. The binding of miR-99a-5p and VLDLR was measured by dual-luciferase reporter gene assay; C. miR-99a-5p and VLDLR enrichment by Ago2 was determined by RIP assay; D. VLDLR expression levels in clinical tissues were measured by RT-qPCR (n = 86); E. VLDLR expression levels in A549/DPP cells and A549 cells were tested by RT-qPCR; F. The effects of miR-99a-5p on VLDLR protein expression were assessed by western blot; $*P < 0.05$.

Inhibition of VLDLR promotes sensitivity to DDP in lung cancer cells

To assess the effects of VLDLR on lung cancer cell sensitivity to chemotherapy, we designed specific siRNAs to knockdown VLDLR expression and measured the interference efficiency of si-VLDLR. A549/DDP cells were transfected with either si-NC or si-VLDLR. RT-qPCR was performed to test VLDLR expression in the transfected cells. The findings demonstrated that VLDLR expression levels were inhibited after si-VLDLR transfection (Figure 4A), indicating that si-VLDLR effectively knocked down VLDLR expression in lung cancer cells.

Next, A549/DDP cell viability after transfection with si-NC and si-VLDLR at different DDP concentrations and measured by the CCK-8 assay, which showed reduced cell viability after si-VLDLR transfection, along with decreased DDP IC_{50} values (Figure 4B).

Additionally, cell proliferation capacity, colony formation capacity, and apoptosis were measured. The experimental results revealed that the cell proliferation and colony formation capacities decreased after transfection with si-VLDLR (Figure 4C-D), while apoptosis increased (Figure 4E). Finally, the expression levels of apoptosis-related genes (Bax, Bcl-2, and caspase-3) were assessed. The results demonstrated that si-VLDLR treatment upregulated Bax and caspase-3 mRNA levels and downregulated Bcl-2 mRNA levels (Figure 4F).
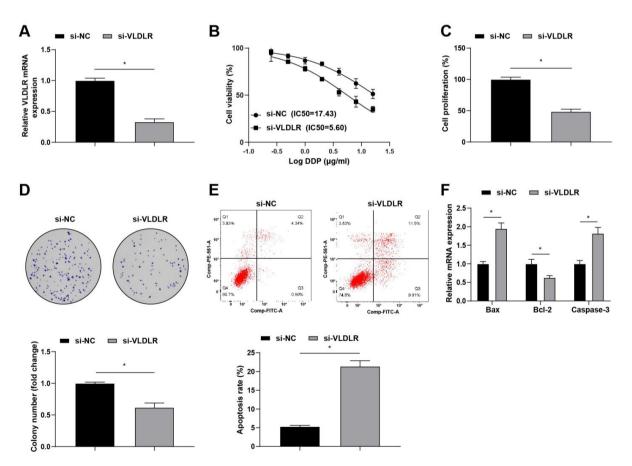

FIGURE 4 - Suppression of VLDLR promotes lung cancer cell chemotherapy sensitivity. A. The interference efficiency of si-VLDLR was measured by RT-qPCR; B. A549/DDP cell viability at different DDP concentrations after transfected with si-VLDLR was tested by CCK-8 assay; C. The cell viability of A549/DDP cells after transfection with si-VLDLR was assessed by CCK-8 assay; D. The colony formation capacity of A549/DDP cells after si-VLDLR transfection was evaluated by colony formation assay; E. A549/DDP cell apoptosis rate after si-VLDLR transfection was assessed by flow cytometry; F. The expression of apoptosis-related genes in A549/DDP cells after si-VLDLR transfection was tested by RT-qPCR; *$P < 0.05$.

The miR-99a-5p/VLDLR axis is linked to lung cancer sensitivity to DDP

To validate the involvement of the miR-99a-5p/VLDLR axis in the chemotherapy sensitivity of lung cancer, we established inhibitor NC + si-NC, miR-99a-5p inhibitor + si-NC, and miR-99a-5p inhibitor + si-VLDLR groups. First, RT-qPCR was performed to assess miR-99a-5p and VLDLR mRNA levels in each group after transfection, which that, in comparison with the inhibitor NC + si-NC group, the miR-99a-5p inhibitor + si-NC and miR-99a-5p inhibitor + si-VLDLR groups exhibited lower miR-99a-5p expression levels. In addition, the miR-99a-5p inhibitor + si-NC group had up-regulated VLDLR expression whereas the miR-99a-5p inhibitor + si-VLDLR group had down-regulated VLDLR expression (Figure 5A). Cell viability was evaluated at different DDP concentrations, and

the findings revealed that cell viability and DDP IC_{50} values were enhanced in the miR-99a-5p inhibitor + si-NC group. The miR-99a-5p inhibitor + si-VLDLR group showed reduced cell viability and decreased DDP IC_{50} values compared with the miR-99a-5p inhibitor + si-NC group (Figure 5B).

Further experiments revealed an increase in cell proliferation and colony formation (Figure 5C-D), a reduction in apoptosis (Figure 5E), reduced Bax and caspase-3 mRNA levels, and elevated Bcl-2 mRNA levels (Figure 5F) in the miR-99a-5p inhibitor + si-NC group compared to those in the inhibitor NC + si-NC group. Compared with the miR-99a-5p inhibitor + si-NC group, the miR-99a-5p inhibitor + si-VLDLR group showed inhibition of cell proliferation and colony formation capacity, increased apoptosis rate, upregulation of Bax and caspase-3 mRNA levels, and the suppression of Bcl-2 mRNA levels (Figure 5C-F).
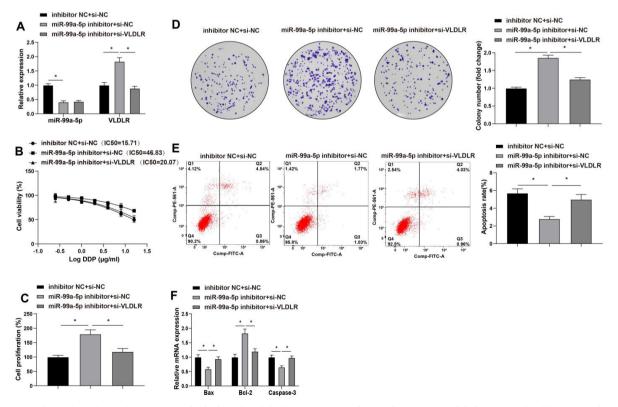

FIGURE 5 - The miR-99a-5p/VLDLR axis is involved in lung cancer chemotherapy sensitivity. A. miR-99a-5p and VLDLR expression levels in the rescue experiment were assessed by RT-qPCR; B. A549/DDP cell viability at different DDP concentrations in the rescue experiment was assessed by CCK-8 assay; C. A549/DDP cell viability in the rescue experiment was measured by CCK-8 assay; D. A549/DDP cell colony formation capacity in the rescue experiment was evaluated by colony formation assay; E. The apoptosis rate of A549/DDP cells in the rescue experiment was assessed by flow cytometry; F. The apoptosis-related gene expression levels in A549/DDP cells in the rescue experiment was tested by RT-qPCR; *$P < 0.05$.

miR-99a-5p overexpression represses the growth of lung cancer transplanted tumors and DDP resistance *in vivo*

miR-99a-5p effects on tumor growth and DDP resistance were verified in nude mice *in vivo* and nude mice transplanted with tumor models were established using A549 cells. A549 cells with stable overexpression of miR-99a-5p or scrambled miRNA were resuspended in PBS and inoculated into nude mice, and abdominal DDP was simultaneously administered to mice after miR-NC + DDP and miR-99a-5p + DDP treatment. The transplanted tumor growth volume was recorded to reflect the transplanted tumor DDP resistance, and the findings revealed that overexpression of miR-99a-5p reduced the transplanted tumor volume in mice, which was further suppressed in the miR-99a-5p + DDP group (Figure 6A-B). Apoptosis in tumor tissues was detected using TUNEL staining, and the results revealed that the number of TUNEL-positive cells increased in the tumor tissues of mice after treatment with miR-99a-5p overexpression, and apoptosis levels were further elevated in mice in the miR-99a-5p + DDP group (Figure 6C). These results suggest that *in vivo* miR-99a-5p overexpression represses the growth of transplanted tumors and DDP resistance in lung cancer.
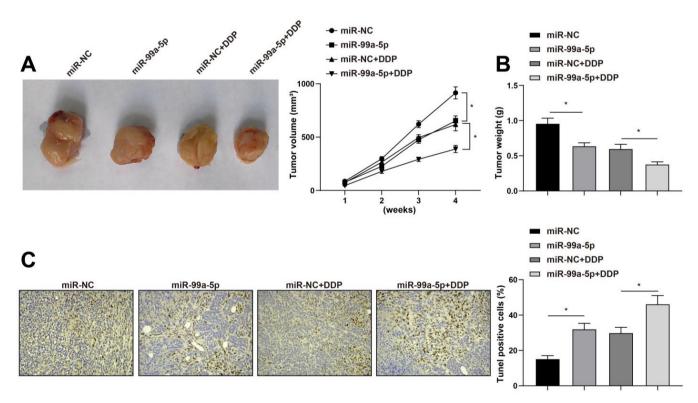

FIGURE 6 - miR-99a-5p overexpression represses the growth of transplanted tumors and cisplatin resistance *in vivo*. A. Representative figures and growth curve of transplanted tumors treated with cisplatin in nude mice; B. Weight of transplanted tumors in nude mice after cisplatin treatment *in vivo*; C. The number of TUNEL-positive cells in transplanted tumors was measured by TUNEL staining; * $P < 0.05$, n = 6 mice.

DISCUSSION

Lung cancer is a frequently diagnosed cancer (Thai *et al.*, 2021) and the main cause of cancer-related mortality (Ruiz-Cordero, Devine, 2020). In this study, we aimed to determine whether miR-99a-5p plays a role in modulating VLDLR to affect lung cancer and discovered that miR-99a-5p overexpression promotes sensitivity

to DDP and cell apoptosis by downregulating VLDLR expression in A549/DDP cells.

The development of DDP resistance is a major problem in cancer chemotherapy (Chen *et al.*, 2015). In addition, changes in the expression of various drug-resistant genes that may be modulated by miRNAs result in drug resistance (Kazmierczak *et al.*, 2022). Moreover, miRNAs can predict lung cancer resistance and sensitivity to DDP. In particular, the selected miRNAs possess high potential in the prediction of lung cancer DDP sensitivity or resistance and in DDP co-therapy development (Konoshenko *et al.*, 2022). In our study, we found that miR-99a-5p was under-expressed in lung cancer, and miR-99a-5p level reduction was associated with poor survival in patients with lung cancer. Previous studies have reported reduced miR-99a expression in CC (Wang *et al.*, 2022). Consistent with our findings, a previous study revealed that decreased miR-99a-5p expression is associated with poor prognosis in LUAD patients (Mizuno *et al.*, 2020). In this study, we found that miR-99a-5p overexpression promotes chemotherapy sensitivity in lung cancer cells and represses lung cancer-transplanted tumor growth and cisplatin resistance *in vivo*. The suppression of miR-99a-5p sensitizes GC cells to DDP (Sun *et al.*, 2020). In addition, miR-99a-5p represses bladder cancer cell viability and restores sensitivity to gemcitabine, and miR-99a-5p overexpression represses gemcitabine-resistant cells *in vivo* (Tamai *et al.*, 2022). miR-99a-5p overexpression inhibited the proliferation of two signet-ring cell carcinoma (SRC) cell lines. Additionally, it was discovered that the expression of miR-99a-5p is associated with cell proliferation. Thus, miR-99a-5p can be considered a diagnostic biomarker for SRC at an early stage or a relevant adverse prognosis in these patients (Saito *et al.*, 2020). A previous study has reported that miR-99a-5p serves as a tumor inhibitor. The upregulation of miR-99a-5p suppresses TSCC1 cell vitality, proliferation, invasion, and migration (Shi *et al.*, 2017).

In the present study, we validated the downstream regulatory mechanism of miR-99a-5p. It was predicted that the miR-99a-5p sequences contained VLDLR-binding sites, and further experiments verified that miR-99a-5 targets and regulates VLDLR. VLDLR expression was significantly reduced in CRC tumors. Furthermore, VLDLR overexpression inhibits CRC cell proliferation and migration (Kim *et al.*, 2017). Silencing

VLDLR represses sphere formation capabilities *in vitro* and cancer development *in vivo* in breast cancer cells. Moreover, VLDLR knockdown can induce a transition from self-renewal to quiescence, and high VLDLR expression in breast cancer tissues is associated with the poor prognosis of patients (Yang *et al.*, 2022). In this study, we found that VLDLR knockdown promotes the sensitivity of lung cancer cells to chemotherapy. In addition, the miR-99a-5p/VLDLR axis is involved in sensitivity to chemotherapy and apoptosis in lung cancer.

In conclusion, this study provides evidence of the regulatory effects of the miR-99a-5p/VLDLR axis on the sensitivity of lung cancer cells to chemotherapy. miR-99a-5p overexpression promotes sensitivity to DDP and apoptosis by downregulating VLDLR expression in A549/DDP cells. Our results suggest a link between miR-99a-5p, VLDLR, and chemoresistance, suggesting a novel concept in lung carcinogenesis. Thus, miR-99a-5p represents a novel modulation strategy for overcoming drug resistance. However, in this study, we only explored the sensitivity of miR-99a-5p overexpression to DDP and its effect on tumor growth, and we will further establish its relationship *in vivo* with VLDLR. In future studies, we plan to investigate whether other miRNAs regulate the involvement of VLDLR in the sensitivity of lung cancer cells to chemotherapy. Moreover, whether miR-99a-5p targets the regulation of the PCSK9/VLDLR signaling pathway will be further validated in future studies.

FUNDING

REFERENCES

Ahn YH, Ko YH. Diagnostic and Therapeutic Implications of microRNAs in Non-Small Cell Lung Cancer. Int J Mol Sci. 2020;21(22):8782.

Ashrafizadeh M, Zarrabi A, Hushmandi K, Hashemi F, Moghadam ER, Owrang M, et al. Lung cancer cells and their sensitivity/resistance to cisplatin chemotherapy:

Role of microRNAs and upstream mediators. Cell Signal. 2021;78:109871.

Cai H, Yang X, Gao Y, Xu Z, Yu B, Xu T, et al. Exosomal MicroRNA-9-3p Secreted from BMSCs Downregulates ESM1 to Suppress the Development of Bladder Cancer. Mol Ther Nucleic Acids. 2019;18:787-800.

Chen Y, Gao Y, Zhang K, Li C, Pan Y, Chen J, et al. MicroRNAs as Regulators of Cisplatin Resistance in Lung Cancer. Cell Physiol Biochem. 2015;37(5):1869-80.

Ding C, Xi G, Wang G, Cui D, Zhang B, Wang H, et al. Exosomal Circ-MEMO1 Promotes the Progression and Aerobic Glycolysis of Non-small Cell Lung Cancer Through Targeting MiR-101-3p/KRAS Axis. Front Genet. 2020;11:962.

El-Hussein A, Manoto SL, Ombinda-Lemboumba S, Alrowaili ZA, Mthunzi-Kufa P. A Review of Chemotherapy and Photodynamic Therapy for Lung Cancer Treatment. Anticancer Agents Med Chem. 2021;21(2):149-161.

Feng LL, Shen FR, Zhou JH, Chen YG. Expression of the lncRNA ZFAS1 in cervical cancer and its correlation with prognosis and chemosensitivity. Gene. 2019;696:105-112.

Gao Y, Wang Y, Chen X, Peng Y, Chen F, He Y, et al. MiR-127 attenuates adipogenesis by targeting MAPK4 and HOXC6 in porcine adipocytes. J Cell Physiol. 2019;234(12):21838-21850.

Garrido-Cano I, Constancio V, Adam-Artigues A, Lameirinhas A, Simon S, Ortega B, et al. Circulating miR-99a-5p Expression in Plasma: A Potential Biomarker for Early Diagnosis of Breast Cancer. Int J Mol Sci. 2020;21(19):7427.

Gu A, Bao X. MiR-99a-5p Constrains Epithelial-Mesenchymal Transition of Cervical Squamous Cell Carcinoma Via Targeting CDC25A/IL6. Mol Biotechnol. 2022;64(11):1234-1243.

He L, Lu Y, Wang P, Zhang J, Yin C, Qu S. Up-regulated expression of type II very low density lipoprotein receptor correlates with cancer metastasis and has a potential link to beta-catenin in different cancers. BMC Cancer, 2010;10:601.

Hwang H, Chang HR, Baek D. Determinants of Functional MicroRNA Targeting. Mol Cells. 2023;46(1):21-32.

Kazmierczak D, Jopek K, Sterzynska K, Nowicki M, Rucinski M, Januchowski R. The Profile of MicroRNA Expression and Potential Role in the Regulation of Drug-Resistant Genes in Cisplatin- and Paclitaxel-Resistant Ovarian Cancer Cell Lines. Int J Mol Sci. 2022;23(1):526.

Kim BK, Yoo HI, Lee AR, Choi K, Yoon SK. Decreased expression of VLDLR is inversely correlated with miR-200c in human colorectal cancer. Mol Carcinog. 2017;56(6):1620-1629.

Konoshenko M, Lansukhay Y, Krasilnikov S, Laktionov P. MicroRNAs as Predictors of Lung-Cancer Resistance and Sensitivity to Cisplatin. Int J Mol Sci. 2022;23(14):7594.

Li J, Zhong X, Zhao Y, Shen J, Pilapong C, Xiao Z. Polyphenols as Lung Cancer Chemopreventive Agents by Targeting microRNAs. Molecules. 2022;27(18):5903.

Liu N, Jiang N, Guo R, Jiang W, He QM, Xu YF, et al. MiR-451 inhibits cell growth and invasion by targeting MIF and is associated with survival in nasopharyngeal carcinoma. Mol Cancer. 2013;12(1):123.

Livak KJ, Schmittgen TD. Analysis of relative gene expression data using real-time quantitative PCR and the 2(-Delta Delta C(T)) Method. Methods. 2001;25(4):402-8.

Luo M, Liu YJ, Xia LM, Yan W, Zhu Q, Tian DA. Very low density lipoprotein receptor subtype II silencing by RNA interference inhibits cell proliferation in hepatoma cell lines. Hepatogastroenterology. 2010;57(101):882-90.

Mizuno K, Tanigawa K, Nohata N, Misono S, Okada R, Asai S, et al. FAM64A: A Novel Oncogenic Target of Lung Adenocarcinoma Regulated by Both Strands of miR-99a (miR-99a-5p and miR-99a-3p). Cells. 2020;9(9):2083.

Ruiz-Cordero R, Devine WP. Targeted Therapy and Checkpoint Immunotherapy in Lung Cancer. Surg Pathol Clin. 2020;13(1):17-33.

Saito R, Maruyama S, Kawaguchi Y, Akaike H, Shimizu H, Furuya S, et al. miR-99a-5p as Possible Diagnostic and Prognostic Marker in Patients With Gastric Cancer. J Surg Res. 2020;250:193-199.

Saliminejad K, Khorram Khorshid HR, Soleymani Fard S, Ghaffari SH. An overview of microRNAs: Biology, functions, therapeutics, and analysis methods. J Cell Physiol. 2019;234(5):5451-5465.

Shi Y, Bo Z, Pang G, Qu X, Bao W, Yang L, et al. MiR-99a-5p regulates proliferation, migration and invasion abilities of human oral carcinoma cells by targeting NOX4. Neoplasma. 2017;64(5):666-673.

Sun G, Li Z, He Z, Wang W, Wang S, Zhang X, et al. Circular RNA MCTP2 inhibits cisplatin resistance in gastric cancer by miR-99a-5p-mediated induction of MTMR3 expression. J Exp Clin Cancer Res. 2020;39(1):246.

Tamai M, Tatarano S, Okamura S, Fukumoto W, Kawakami I, Osako Y, et al. microRNA-99a-5p induces cellular senescence in gemcitabine-resistant bladder cancer by targeting SMARCD1. Mol Oncol. 2022;16(6):1329-1346.

Tang C, Yang H, Zhou X. [Advances of DNA damage repair and Cisplatin resistance mechanisms in lung cancer]. Zhongguo Fei Ai Za Zhi. 2011;14(12):960-4.

Teng JP, Yang ZY, Zhu YM, Ni D, Zhu ZJ, Li XQ. Gemcitabine and cisplatin for treatment of lung cancer in vitro and vivo. Eur Rev Med Pharmacol Sci. 2018;22(12):3819-3825.

Thai AA, Solomon BJ, Sequist LV, Gainor JF,. Heist RS. Lung cancer. Lancet. 2021;398(10299):535-554.

Thakur SK, Singh DP, Choudhary J. Lung cancer identification: a review on detection and classification. Cancer Metastasis Rev. 2020;39(3):989-998.

Wang G, Lu Y, Di S, Xie M, Jing F, Dai X. miR-99a-5p inhibits glycolysis and induces cell apoptosis in cervical cancer by targeting RRAGD. Oncol Lett. 2022;24(1):228.

Xie H, Yao J, Wang Y, Ni B. Exosome-transmitted circVMP1 facilitates the progression and cisplatin resistance of non-small cell lung cancer by targeting miR-524-5p-METTL3/SOX2 axis. Drug Deliv. 2022;29(1):1257-1271.

Yang M, Zhan Y, Hou Z, Wang C, Fan W, Guo T, et al. VLDLR disturbs quiescence of breast cancer stem cells in a ligand-independent function. Front Oncol. 2022;12:887035.

Yang SJ, Huang CH, Wang CH, Shieh MJ, Chen KC. The Synergistic Effect of Hyperthermia and Chemotherapy in Magnetite Nanomedicine-Based Lung Cancer Treatment. Int J Nanomedicine. 2020;15:10331-10347.

Yu X, Shi W, Zhang Y, Wang X, Sun S, Song Z, et al. CXCL12/CXCR4 axis induced miR-125b promotes invasion and confers 5-fluorouracil resistance through enhancing autophagy in colorectal cancer. Sci Rep. 2017;7:42226.

Yu XY, Jin X, Shou ZX. Surface-engineered smart nanocarrier-based inhalation formulations for targeted lung cancer chemotherapy: a review of current practices. Drug Deliv. 2021;28(1):1995-2010.

Zheng D, Zhu Y, Zhang J, Zhang W, Wang H, Chen H, et al. Identification and evaluation of circulating small extracellular vesicle microRNAs as diagnostic biomarkers for patients with indeterminate pulmonary nodules. J Nanobiotechnology. 2022;20(1):172.

Yaoguo Lang, Xianglong Kong, Benkun Liu, Xiangyuan Jin, Lantao Chen, Shidong Xu

SUPPLEMENTARY

TABLE I - The primer sequences for RT-qPCR

	Forward Primer (5′-3′)	Reverse Primer (5′-3′)
miR-99a-5p	**AACCCGTAGAT**CCGATCTTGTG	**mRQ 3′ Prim**er
U6	**GCTTCGGCAGC**ACATATACTAAAAT	**CGCTTCACGAA**TTTGCGTGTCAT
VLDLR	**CTAGTCAACAA**CCTGAATGATG	**AAGAATGGCCC**ATGCGGCAGAA
Bax	**CACCAGCTCTG**AACAGATCATGA	**TCAGCCCATCT**TCTTCCAGATGGT
Bcl2	**GAGGATTGTGG**CCTTCTTTG	**AGCCTGCAGCT**TTGTTCCAT
caspase-3	**GGTGTTGATGA**TGACATGGCG	**GTACCCTCTGC**AGCATGAGAGTAG
β-actin	**CACTCTTCCAG**CCTTCCTTCC	**CGGACTCGTCA**TACTCCTGCTT

Note: miR-99a-5p, microRNA-99a-5p; VLDLR, very-low-density-lipoprotein receptor.